Assessment of scour depth around offshore monopile foundation under varying hydrodynamic conditions with influence of material state

A. Jatoliya[1], D. Bhattacharya[2], B. Manna[3] and T. F. Ferradosa[4]

[1,2,3] Department of Civil and Environmental Engineering, Indian Institute of Technology Delhi, Hauz Khas, New Delhi – 110016, India,

Email: cez218267@iitd.ac.in, debayanb@iitd.ac.in, bmanna@iitd.ac.in

[4] Department of Civil Engineering, Faculty of Engineering of the University of Porto, Rua Dr. Roberto Frias, s/n, 4200-465, Porto, Portugal, Email: tiago.ferradosa@fe.up.pt

[*] *Ajay.Jatoliya@civil.iitd.ac.in (corresponding author)*

ABSTRACT: Offshore Wind Turbines (OWT) have emerged as a key technology for achieving clean and sustainable energy. However, accurate assessment of scour depth around these offshore foundations is crucial for maintaining structural integrity and long-term operational reliability. In the present study, we employ numerical experiments to assess the scour depth around the monopile foundation under varying hydrodynamic conditions, namely: current-only, wave-only, and coupled wave-current conditions. Additionally, the effect of base material porosity (n) on the scour depth was investigated. Flow dynamics around these structures are resolved by solving the Reynolds-Averaged Navier–Stokes (RANS) equations in conjunction with the continuity equation for incompressible fluids, that can resolve the interaction between the flow hydrodynamics and sediment transport phenomena. The flow behaviour was analysed by investigating the velocity vectors and streamline patterns. Outcomes of the present study reveal that the flow behaviour around the monopile foundation is more complex in case of wave only condition as compared to the steady flow condition. Furthermore, it was observed that base material density (n) also has a significant effect on the formation of the scour depth. Loosely packed sediment results in a deeper scour depth as compared to densely packed sediments, highlighting the critical influence of material state on seabed erosion dynamics.

Keywords: offshore foundations, scour depth, hydrodynamic conditions, sustainable energy, flow behaviour

1 INTRODUCTION

Offshore Wind Turbines (OWT) play a crucial role in the development and global shift towards sustainable energy. These structures provide a robust and renewable source of electricity with minimal greenhouse gas emissions. Positioned in open-sea locations, these critical energy infrastructure units offer more robust and consistent wind speeds than their onshore counterparts, thus allowing them to generate substantial energy to meet the ever-growing demands of urban and industrial regions (Jatoliya et al., 2024). However, deployment of these large-scale structures in marine environments poses several engineering challenges; one of the most critical being the seabed scour phenomenon around their foundations (Fazeres-Ferradosa et al., 2021). Scouring refers to the erosion of seabed sediments caused by the formation of eddy currents due to waves, currents, or their combined action (Wilcox, 2006). This process can lead to a substantial lowering of the seabed level around the foundation, compromising the structural stability and service life of the wind turbine (Díaz & Guedes Soares, 2020). Accurate prediction and assessment of scour depth are therefore extremely essential for the safe and cost-effective design of offshore wind turbine foundations. Various foundation types, such as monopile, tripile, suction caisson, and gravity-based structures, can be found in literature that have been employed in offshore wind farms depending on water depth, soil conditions, and economic considerations (Bhattacharya et al., 2020). Among these, the monopile foundations are widely adopted due to their structural simplicity and ease of installation. However, their hydrodynamic behaviour and corresponding scour patterns differ significantly due to variations in flow interference, vortex formation, and sediment transport mechanisms (Baykal et al., 2015). Previous experimental and numerical studies have investigated scour processes around monopile foundations (Baranwal et al., 2023; Melville, 1975; Quezada et al., 2019; Zhang et al., 2017) . However, comparatively very few studies have focused on the formation of the scour depth while considering the systematic effect of the material state under realistic hydrodynamic conditions. Moreover, the influence of sediment characteristics particularly porosity (*n*) on scour development remains insufficiently understood. The present study aims to address these gaps by performing careful numerical simulations to evaluate the scour depth around monopile foundations under varying hydrodynamic conditions, including current-only, wave-only, and coupled wave–current scenarios and the effect of the material state. The flow dynamics is modelled using the Reynolds-Averaged Navier–Stokes (RANS) equations coupled with the continuity equation for incompressible fluids, allowing for accurate representation of flow sediment interactions. The study further investigates the effects of sediment properties on scour evolution to enhance understanding of seabed erosion processes and support the design of stable offshore wind turbine foundations.

2 NUMERICAL MODELING

The present research employs the open-source framework REEF3D (Bihs et al., 2016), based on the three-dimensional (3D) Computational Fluid Dynamics (CFD) method to model the wave-structure interaction. It can solve semi-coupled, including two-phase and three-phase problems, utilizing the level set method to distinguish between these phases. This model addresses the fluid flow problem using the incompressible Reynolds-averaged Navier-Stokes (RANS) equations in conjunction with the continuity equation, as illustrated by Equations (1) and (2) (Chorin, 1968).

$$\frac{\partial u_i}{\partial x_i} = 0 \qquad (1)$$

$$\frac{\partial U_i}{\partial t} + U_j \frac{\partial U_i}{\partial x_j} = -\frac{1}{\rho}\frac{\partial P}{\partial x_i} + \frac{\partial\left[(\vartheta + \vartheta t)\left(\frac{\partial U_i}{\partial x_j} + \frac{\partial U_j}{\partial x_j}\right)\right]}{\partial x_j} + g_i \qquad (2)$$

where u_i is the flow velocity, P is the pressure, ρ is the density of the fluid, ν is the kinematic viscosity, v_t is the viscosity, and g represents the gravitational acceleration. The projection method (Chorin, 1968) calculates the pressure generated inside the flow field around the structure in consideration with the help of the BICGStab solver (Jiang & Peng, 2000). The Hamilton–Jacobi equation is employed using a fifth-order Weighted Essentially Non-Oscillatory (WENO) scheme, while the temporal and spatial discretisation of the momentum and level-set numerical schemes is solved using a third-order Runge–Kutta method (Shu & Oshert, 1989). To solve the eddy-viscosity term in the RANS equation $k - \omega$ turbulence model (Wilcox, 1993) is used. The Finite Difference Method (FDM) is uniformly applied to the Cartesian grid to approximate the spatial derivatives in the RANS equation employed in this present investigation.

2.1 Numerical setup and wave generation

The numerical simulations for the assessment of the scour depth were carried out within a three-dimensional (3D) Numerical Wave Tank (NWT). The side and top boundaries of the NWT are specified as symmetric Boundary Conditions (BC), while the bottom boundary is assigned a no-slip condition as depicted in Figure 1 (c).

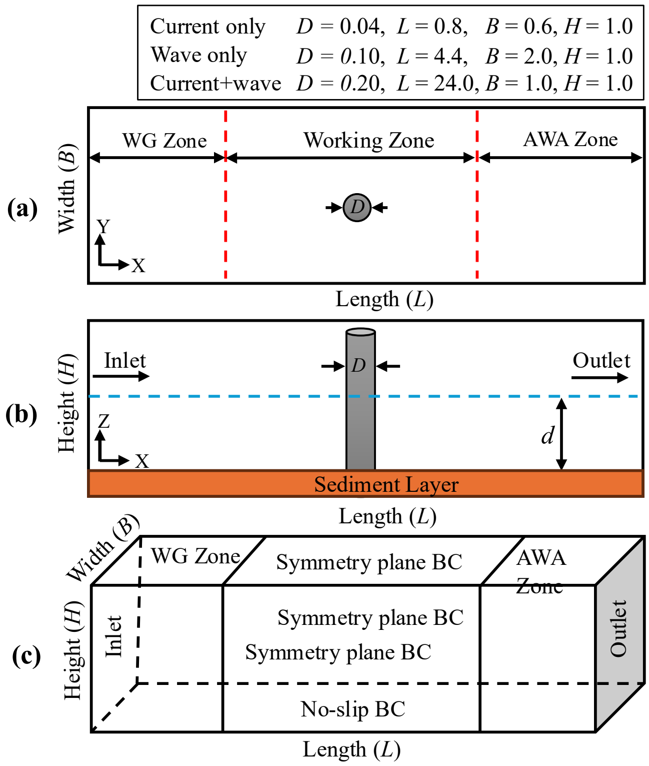

Figure 1. Schematic representation of the computational domain and applied boundary conditions (a) Top view, (b) Sectional view, (c) Isometric view

We carried out these numerical experiments a High-Performance Computing (HPC) facility, and the results were analysed on a Intel Xeon® W-2275 processor with 14 cores operating at 3.30 GHz. Figure 1 (a) depicts the location of the monopile foundation and different zones define in the NWT. To generate the current, waves and coupled waves and current scenario, a Wave Generation (WG) and Active Wave Absorption (AWA) Boundary Condition (BC) are specified at the inlet and outlet of the NWT, respectively. The lengths of these two zones are one and two times the wavelength of the waves, respectively, as shown in Figure 1 (a). The AWA boundary condition is specified to prevent the superimposition of the incident and the reflected waves. Fifth-order cnoidal wave theory was adopted for wave generation, as it accurately represents long-period waves in shallow water, ensuring a realistic prediction of wave kinematics (Ahmad et al., 2018). To capture the wave profile of the generated waves, two wave probes are positioned at the free surface, located at a distance of 1*D* upstream and downstream of the structure.

2.2 Material

For scour depth investigation, cohesionless sediment was used in the present study. The selected material has a mean particle size (d_{50}) of 2.58 mm with particle density (ρ_s) of 2650 kg/m³. In order to examine the influence of sediment packing, three different material states of the soil, loose, medium and dense, were considered (Ahmed et al., 2023). Table 1 summarises the soil properties corresponding to different material states adopted in the present study.

Table 1. Soil parameters used in the present study

Material state	Void Ratio (*e*)	Porosity (*n*)	Angle of repose (ϕ')
Loose	0.75	0.43	33.8^0
Medium	0.69	0.41	39.7^0
Dense	0.62	0.38	43.1^0

3 RESULTS AND DISCUSSION

3.1 Numerical Validation

In this section, the numerical results obtained from the model validation are presented. To assess the numerical accuracy of the REEF3D model, numerical simulations were performed in a rectangular flume with dimensions of 0.8 m in length, 0.6 m in width, and 0.2 m in depth, consistent with the configuration recommended by Baykal et al., (2015). The flume was filled with water to a depth of 0.08 m overlying a uniform sediment bed of thickness 0.12 m, with a median particle size of d_{50} = 0.17 mm. A cylindrical pile having diameter of *D* = 0.04 m was placed at the centre of the domain, while a constant discharge of 0.02 m³ s⁻¹ was imposed at the inlet throughout the entire simulation period. Baykal et al. (2015) reported the temporal evolution of the maximum normalized scour depth (*S/D*) under uniform flow conditions for a simulation duration of 120 s, at both upstream and downstream locations of the pile. The results obtained from the REEF3D simulations shows good agreement with the results reported by the Baykal et al., (2015) at the upstream and downstream region as depicted in Figure 2. The dimensionless scour depths (S/D) predicted by REEF3D were 0.86 upstream and 0.71 downstream, closely matching the values of 0.91 and 0.73 reported by (Baykal et al., 2015).

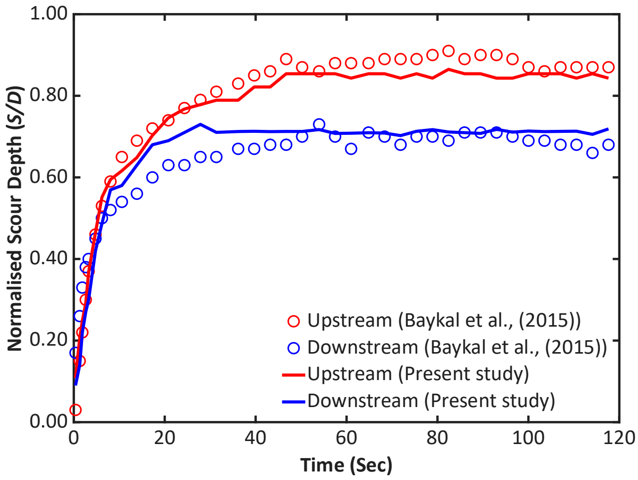

Figure 2. Numerical validation of REEF3D model against the existing studies reported by Baykal et al., (2015) at the upstream and downstream locations of a monopile under steady flow conditions for monopile

3.2 Assessment of scour depth

The virtual experiments were carried out to investigate the effect of material porosity (*n*) on the scour development around a monopile foundation under varying hydrodynamic conditions, namely: current only, wave only, and coupled wave and current environments. To investigate this three different material porosity, loose sand with *n* = 0.43, medium sand with *n* = 0.41 and dense sand with *n* = 0.38 were adopted in the present study. For all three hydrodynamic conditions, the dimensions of the NWT were adjusted to ensure numerical stability, and the corresponding domain configurations are depicted in Figure 1. For the steady current condition, the NWT domain and other flow parameters has been adopted from the previous study reported by (Quezada et al., 2018). The flow was initialised with a uniform water depth of 0.6 m and a flow velocity of 0.60 m/s.

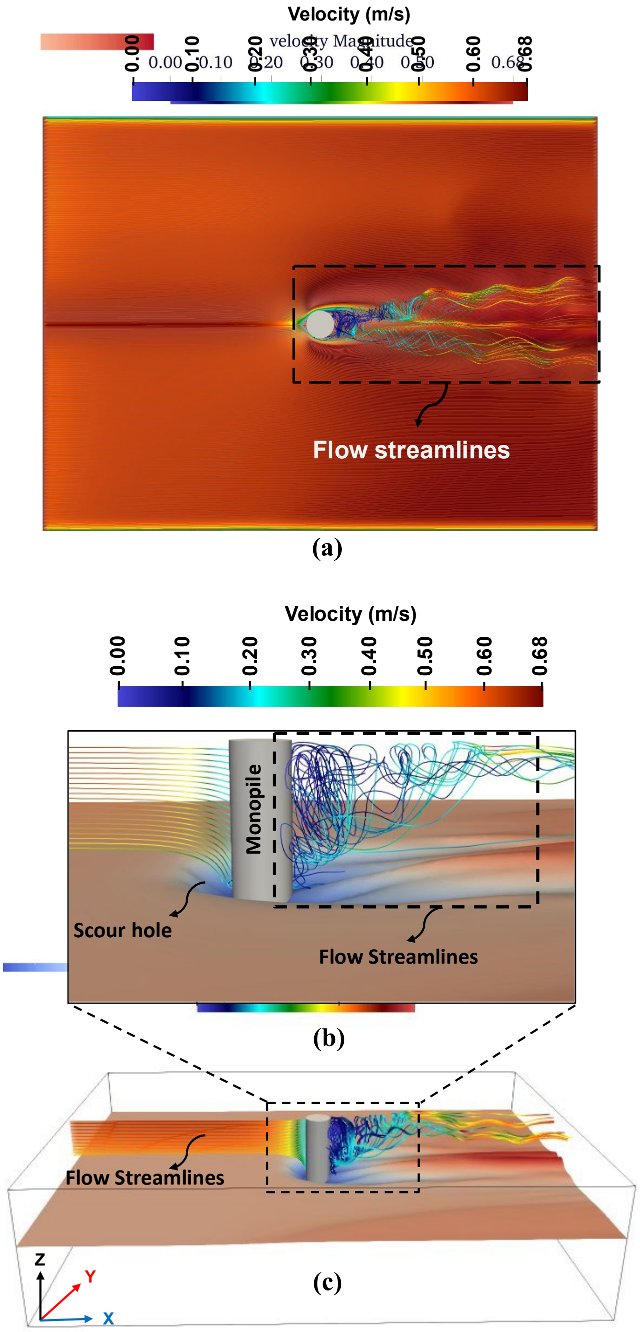

Figure 3. (a) Top view of the velocity flow field (b) Formation of the streamlines around the monopile (c) Iso metric view of the streamlines along with scour hole formation

For numerical stability and accuracy of the model, a uniform structured grid with equal spacing in all spatial directions was employed for the current-only condition. The grid resolution was maintained as $dx = dy = dz = 0.005$ m, resulting in a total of 7,68,000 computational cells in the domain and a physical simulation time of 120 s was adopted, consistent with previously reported studies (Quezada et al., 2018). Corresponding to the flow velocity, the measured resulting Shields parameter (θ) was around 0.135, slightly exceeding the critical shield value ($\theta_{cr} \approx 0.0406$) required for initiating sediment motion (Soulsby & Whitehouse, 1997). To measure the maximum scour depth around the monopile no specific location is predefined before and after the monopile. However, the scour field is assessed over the entire influence zone surrounding the monopile, and the maximum scour depth is determined by identifying the minimum bed elevation. From the figure 4 (b) it is observed that the maximum scour depth is formed at the upstream side of the monopile and deposition occur at the downstream side of the monopile. Figure 3 (a) illustrates the top view of the velocity flow field and the associated streamline patterns at the upstream and downstream faces of the monopile foundation. Formation of these streamlines play a key role in initiating sediment mobilisation, which ultimately leads to the development of scour around the monopile foundation. As evident from Figures 3 (b) and 3 (c), the flow velocity magnitude just before at the upstream face of the monopile is approximately 0.35 m/s due to flow stagnation. As the flow passes through the monopile As a result, the mean velocity of the streamlines decreases in the wake of the monopile compared to the upstream and lateral regions. This velocity deficit persists until the flow gradually recovers further downstream. Figure 4 (a) illustrates the temporal evaluation of the normalised scour depth (S/D) where S is the scour depth, D is the pile diameter for the current only condition, considering the three different material states: loose, medium and dense sand, respectively. From the illustration (Fig. 4 (a)), it was observed that as soil density increases, the scour depth decreases. For loose sand ($n = 0.43$), the observed normalised scour depth (S/D) was approximately 0.849, whereas for medium sand ($n = 0.41$) and dense sand ($n = 0.38$) conditions, it was approximately 0.821 and 0.819, respectively. Compared to loose sand, the normalised scour depth is reduced by approximately 3.30% for medium-dense sand and 3.53% for dense sand. This indicates that for the loose sand ($n = 0.43$), the scour depth is significantly higher due to the easier removal of particles and reduced inter-particle friction. As sediment density increases, particle packing becomes tighter, resulting in enhanced frictional resistance, higher effective stress, and a corresponding increase in the critical shear stress required for sediment motion.

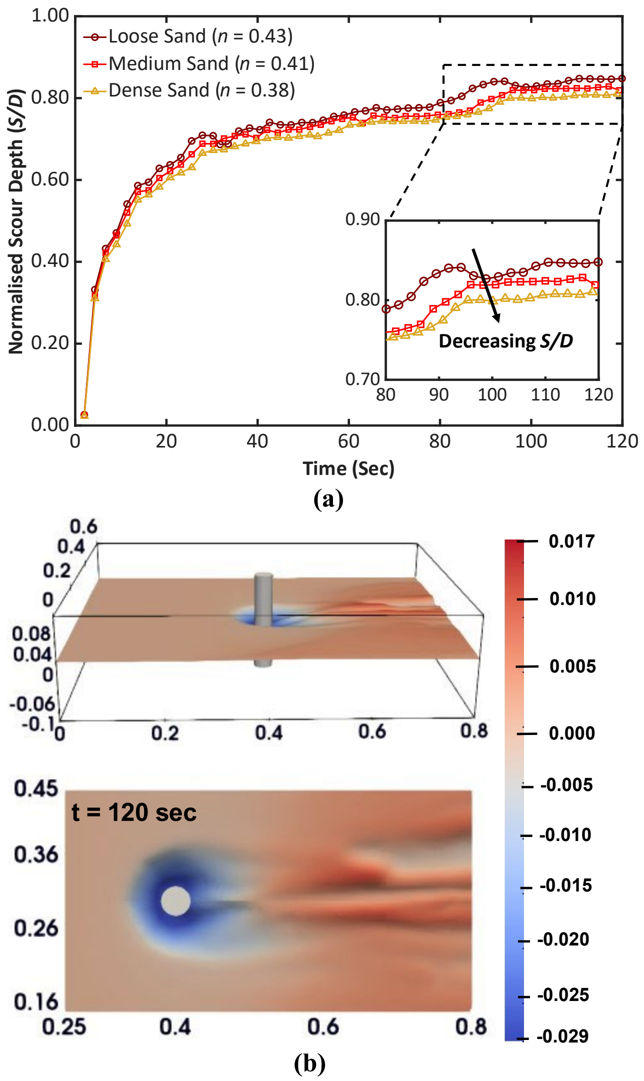

Figure 4. (a) Normalised scour depth (S/D) vs. time (t) plot for monopile under current-only condition, (b) Formation of scour hole around the monopile for loose sand (n = 0.43)

Figure 4 (b) illustrate the formation of the scour depth around the monopile foundation for the current only condition. From the illustration, it can be observed that the maximum scour depth at the upstream toe, while the sediment redeposition occurs at the downstream side of the monopile. For the wave-only condition, an oscillatory flow with a wave height of H = 0.12 m and wave period of T = 4.5 s was applied over a different domain as mentioned earlier in Figure 1, ensuring sufficient space for the wave propagation and boundary dissipation. For numerical stability and accuracy of the model, a uniform structured grid with equal spacing in all spatial directions was employed. The grid resolution was maintained as $dx = dy = dz$ = 0.02 m, resulting in a total of 5,76,000 computational cells in the domain and a physical simulation time of 3600 s was adopted, consistent with previously reported studies (Ahmad et al., 2018). For the wave-only condition, the corresponding maximum near-bed orbital velocity u_m was approximately 0.32 m/s, resulting in a lower shield number (θ = 0.079) as compared to the current-only condition. However, this shield number exceeds the critical shield value ($\theta_{cr} \approx$ 0.0406) required to initiate sediment motion. In the wave-only condition, the periodic reversal of flow direction caused alternating erosion and partial backfilling near the pile, resulting in a more symmetric scour profile compared with the steady current case.

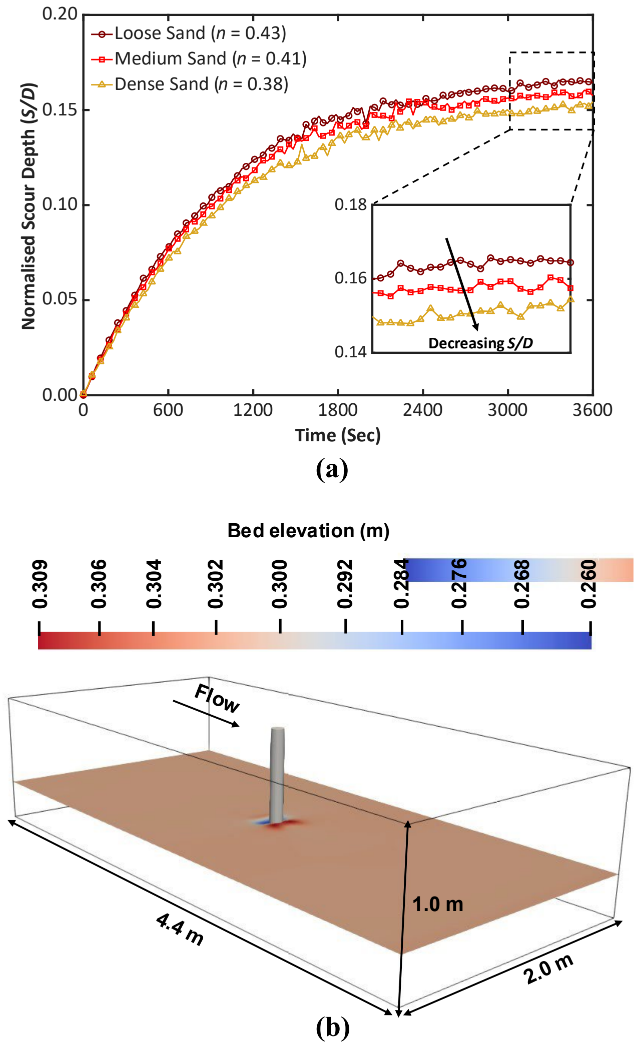

Figure 5. (a) Normalised scour depth (S/D) vs. time (t) plot for monopile under wave-only condition, (b) formation of the scour hole around the monopile due to wave-only condition for loose sand (n = 0.43)

Figure 5 (a) depicts the temporal evaluation of the normalised scour depth (S/D) for the wave-only condition, considering three material states: loose sand

(n = 0.43), medium sand (n = 0.41) and dense sand (n = 0.38). The results indicate that scour depth decreases as sediment density increases, following a similar trend discussed earlier in this section. From the results, it is observed that normalised scour depth (*S/D*) for loose sand (n = 0.43) was approximately 0.164, whereas for medium sand (n = 0.41) and dense sand (n = 0.38), it was around 0.158 and 0.152, respectively. Compared to loose sand, the normalised scour depth is reduced by approximately 3.66% for medium sand and 7.32% for dense sand. This trend can be attributed to the lower resistance to particle motion in loose sand (n = 0.43), where reduced inter-particle friction facilitates sediment removal. In contrast, medium (n = 0.41) and dense (n = 0.38) sands exhibit tighter particle packing, higher effective stress, and increased critical shear stress, resulting in lower scour depths under wave action. Whereas the maximum scour depth in the case of only wave condition is lower than that of the steady current scenario, as sediment redeposition occurs during each wave cycle and due to lower orbital velocity (u = 0.32 m/s) as compared to steady current velocity (u = 0.60 m/s). Figure 5 (b) depicts the formation of the scour depth around the monopile foundation due to wave only condition. For the combined current-wave condition, another domain of NWT is chosen to avoid the numerical instability issues, as shown in Figure 1. Similarly a uniform structured grid with equal spacing in all spatial directions was employed. The grid resolution was maintained as $dx = dy = dz = 0.01$ m, resulting in a total of 30,00,000 computational cells in the domain and a physical simulation time of 1800 s was adopted, consistent with previously reported studies (Quezada et al., 2019). The In the NWT, a steady current with a current velocity of u = 0.21 m/s was superimposed with waves of wave height H = 0.12 m and wave period of T = 4.5 s. This combined flow yielded a Shields parameter of approximately 0.086, well above the threshold critical shield number ($\theta_c \approx 0.0406$) for sediment motion. Figure 5 (a) illustrates the normalised scour depth (*S/D*) vs time plot for the combined wave-current condition for the loose, medium-dense and dense sand material states. From the results, it is observed that normalised scour depth (*S/D*) for loose sand (n = 0.43) was approximately 0.177, whereas for medium sand (n = 0.41) and dense sand (n = 0.38), it was around 0.173 and 0.170, respectively. The results demonstrate that scour depth decreases with increasing sediment density. Compared to loose sand, the normalised scour depth is reduced by about 2.26% for medium sand and 3.95% for dense sand. Figure 5 (b) shows the formation of the scour depth near the monopile foundation under a combined wave current environment. In the coupled wave-current environment.

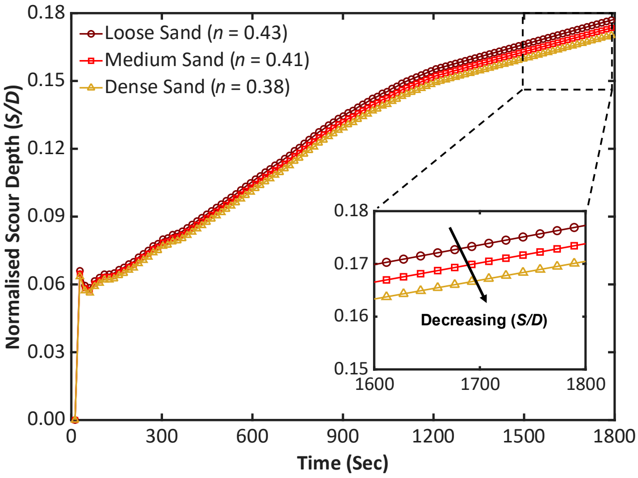

(a)

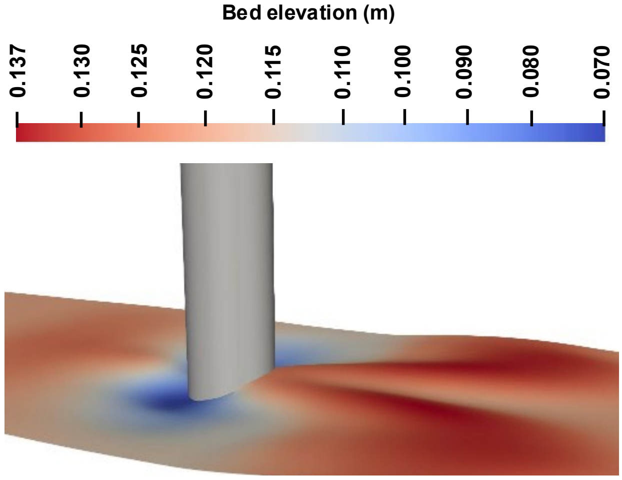

(b)

Figure 6. (a) Temporal evaluation of Normalized scour depth (*S/D*) for monopile foundation under coupled wave and current condition (b) Formation of the scour hole around the monopile foundation due to coupled wave and current environment for loose sand (n = 0.43)

4 CONCLUSIONS

The present numerical investigation presents a comprehensive assessment of the temporal evolution of scour depth around a monopile foundation subjected to three hydrodynamic conditions: steady current, wave-only, and combined wave-current scenarios, for a cohesionless sediment with a median grain size of d_{50} = 2.58 mm. To examine the influence of material state on scour development, three material states were considered: loose sand (n = 0.43), medium sand (n = 0.41), and dense sand (n = 0.43). Under the current only condition, the normalised scour depth (*S/D*) was observed to be 0.849, 0.821, and 0.819 for loose, medium, and dense sand, respectively. Relative to loose sand, this corresponds to a reduction of approximately 3.30% for medium sand and 3.53% for dense sand. For the wave-only condition, the normalised scour depths (*S/D*) were significantly lower, with values of 0.164, 0.158, and 0.152 for loose, medium, and dense sand, respectively, representing reductions of 3.66% and 7.32% for medium and dense sands compared to loose sand. In the combined wave–current condition, the normalised scour depths increased to 0.177, 0.173, and 0.170 for loose, medium, and dense sand, respectively, corresponding to reductions of 2.26% and 3.95% relative to loose sand. These results demonstrate that although sediment densification consistently reduces scour depth under all flow regimes, the hydrodynamic condition plays a dominant role in determining scour severity. Overall, the findings confirm that scour around monopile foundations is highly sensitive to both sediment state and hydrodynamic regime. While denser sediments mitigate scour through increased inter-particle friction and higher critical shear stress, stronger flow conditions significantly amplify erosion. These results highlight the importance of incorporating realistic combinations of flow conditions and soil properties in the design and assessment of offshore monopile-supported structures to ensure long-term stability and performance. The results also demonstrate that for the motion of the bed particles, the flow and orbital velocity should be more than the critical flow velocity, which is measured using the critical shield number. These findings highlight the necessity of incorporating realistic hydrodynamic loading and soil conditions in the design and assessment of offshore monopile-supported structures to ensure long-term stability and performance.

AUTHOR CONTRIBUTION STATEMENT

Ajay Jatoliya: Conceptualization, data analysis, software, formal investigation, methodology, investigation, original draft writing, and visualisation. **Debayan Bhattacharya**: Conceptualization, investigation, data management, methodology development, formal analysis, supervision, project administration, resource allocation, review, and editing. **Bappaditya Manna**: supervision, project administration, resource allocation, review, and editing. **Tiago Fazeres Ferradosa:**, supervision, administration, reviewing and editing.

ACKNOWLEDGEMENTS

The first author acknowledges sincere gratitude to the Ministry of Education, India, for the financial support, High-Performance Computing (HPC) facility and material resources provided by IIT Delhi. The second author acknowledges sincere gratitude for the Seed Grant Fund received from IIT Delhi, and the third author acknowledges the funds received from Research Design and Standards Organization (RDSO) project no. RP04252G.

REFERENCES

Ahmad, N., Bihs, H., Myrhaug, D., Kamath, A., & Arntsen, Ø. A. (2018). Three-dimensional numerical modelling of wave-induced scour around piles in a side-by-side arrangement. *Coastal Engineering*, *138*. https://doi.org/10.1016/j.coastaleng.2018.04.016

Ahmed, S. S., Martinez, A., & DeJong, J. T. (2023). Effect of Gradation on the Strength and Stress-Dilation Behavior of Coarse-Grained Soils in Drained and Undrained Triaxial Compression. *Journal of Geotechnical and Geoenvironmental Engineering*, *149*(5). https://doi.org/10.1061/jggefk.gteng-10972

Baranwal, A., Shankar Das, B., & Setia, B. (2023). A comparative study of scour around various shaped bridge pier. *Engineering Research Express*, *5*(1). https://doi.org/10.1088/2631-8695/acbfa1

Baykal, C., Sumer, B. M., Fuhrman, D. R., Jacobsen, N. G., & Fredsoe, J. (2015). Numerical investigation of flow and scour around a vertical circular cylinder. *Philosophical Transactions of the Royal Society A: Mathematical, Physical and Engineering Sciences*, *373*(2033). https://doi.org/10.1098/rsta.2014.0104

Bhattacharya, S., Nikitas, G., Aleem, M., Cui, L., Wang, Y., Jalbi, S., & Hilton, J. (2020). Challenges in the design and construction of offshore wind turbine foundations including sites in seismic areas. *Lecture Notes in Civil Engineering*, *92*. https://doi.org/10.1007/978-981-15-6832-9_6

Bihs, H., Kamath, A., Alagan Chella, M., Aggarwal, A., & Arntsen, Ø. A. (2016). A new level set numerical wave tank with improved density interpolation for complex wave hydrodynamics. *Computers and Fluids*, *140*. https://doi.org/10.1016/j.compfluid.2016.09.012

Chorin, A. J. (1968). Numerical Solution of the Navier-Stokes Equations. *Mathematics of Computation*, *22*(104). https://doi.org/10.2307/2004575

Díaz, H., & Guedes Soares, C. (2020). Review of the current status, technology and future trends of offshore wind farms. In *Ocean Engineering* (Vol. 209). https://doi.org/10.1016/j.oceaneng.2020.107381

Fazeres-Ferradosa, T., Chambel, J., Taveira-Pinto, F., Rosa-Santos, P., Taveira Pinto, F. V. C., Giannini, G., & Haerens, P. (2021). Scour protections for offshore foundations of marine energy harvesting technologies: A review. In *Journal of Marine Science and Engineering* (Vol. 9, Number 3). https://doi.org/10.3390/jmse9030297

Jatoliya, A., Bhattacharya, D., Manna, B., Bento, A. M., & Fazeres Ferradosa, T. (2024). Physics-based and machine-learning models for accurate scour depth prediction. *Philosophical Transactions of the Royal Society A: Mathematical, Physical and Engineering Sciences*, *382*(2264). https://doi.org/10.1098/rsta.2022.0403

Jiang, G. S., & Peng, D. (2000). Weighted ENO schemes for Hamilton-Jacobi equations. *SIAM Journal on Scientific Computing*, *21*(6). https://doi.org/10.1137/S106482759732455X

Melville, B. (1975). *Local Scour at Bridge Sites*.

Quezada, M., Tamburrino, A., & Niño, Y. (2018). Numerical simulation of scour around circular piles due to unsteady currents and oscillatory flows. *Engineering Applications of Computational Fluid Mechanics*, *12*(1). https://doi.org/10.1080/19942060.2018.1438924

Quezada, M., Tamburrino, A., & Niño, Y. (2019). Numerical study of the hydrodynamics of waves and currents and their effects in pier scouring. *Water (Switzerland)*, *11*(11). https://doi.org/10.3390/w11112256

Shu, C. W., & Oshert, S. (1989). Efficient implementation of essentially non-oscillatory shock-capturing schemes, II. *Journal of Computational Physics*, *83*(1). https://doi.org/10.1016/0021-9991(89)90222-2

Soulsby, R. L., & Whitehouse, R. J. S. (1997). Threshold of sediment motion in coastal environments. *Proceedings Pacific Coasts and Ports 1997 Conference*, *1*(c).

Wilcox, D. (2006). *Turbulence Modeling for CFD (Third Edition) (Hardcover)*.

Wilcox, D. C. (1993). Turbulence modeling for CFD. In *Aiaa*.

Zhang, Q., Zhou, X. L., & Wang, J. H. (2017). Numerical investigation of local scour around three adjacent piles with different arrangements under current. *Ocean Engineering*, *142*. https://doi.org/10.1016/j.oceaneng.2017.07.045